Spatially localized microwave discharge in the atmosphere as a source of sound

V. A. Zhil'tsov, A. A. Skovoroda, and A. V. Timofeev

"Kurchatov Institute" Russian Scientific Center, 123182 Moscow, Russia

The acoustic properties of a microwave discharge in the atmosphere in the form of a localized plasma (LP) are investigated. Sound modulation associated with modulation of the microwave power is studied. The properties of the phenomenon are explained in terms of a model of a spherically symmetric LP with a thin interface between the plasma and the cold gas. © 1994 American Institute of Physics.

1. INTRODUCTION

Plasma phenomena at atmospheric pressure arouse great interest and are the subject of many investigations, not only in connection with atmospheric electricity but also in view of a multitude of industrial applications. For example, steady discharges of atmospheric pressure are widely employed in arcs, hf discharges, and microwave plasmatrons.[1-4] Because of the absence of electrodes, microwave discharges in the atmosphere have regularly attracted the attention of those investigating ball lightning. In this connection we recall the ideas and experiments of Kapitsa,[5] the work of Finkelstein[6] Handel's hypothesis,[7] and the experiments of Ohtsuki.[8]

In the present work we investigate experimentally and theoretically the acoustic properties of spherical microwave discharges in the quiescent atmosphere which are spatially localized (their dimension is substantially less than that of the discharge chamber). We refer to these as localized plasmas (LP). Similar discharges are described in Ref. 8.

It is known from experience that steady discharges in the atmosphere are generally accompanied by acoustic phenomena (rumbling, crackling, etc.). Discharges in the form of LPs are no exception. Scientific interest in investigating the acoustic properties of LPs results on the one hand from the use of sound as an LP diagnostic and on the other from the possibility of acting on LPs. While the possibility of acoustic diagnostics of, e.g., LP temperature has long been recognized,[9] the effect of sound on the discharge properties has in fact not been studied.[10] The use of an LP as a sound source may be of practical interest also, since it contains no moving mechanical parts.

In Sec. 2 we briefly describe the experimental apparatus, the basic properties of LPs, the technique for exciting sound, and the diagnostics used. The third (theoretical) section is devoted to analyzing sound excitation through modulation of the microwave power supplied. In Sec. 4 we present the experimental data on sound excitation in the range from 50–20000 Hz and compare them with the theory.

2. EXPERIMENTAL APPARATUS

Figure 1 shows a schematic of the device, which essentially reproduces the experiment of Ohtsuki:[8] the frequency of the cw magnetron is 2.45 GHz, the maximum power is 5 kW, and the dimensions of the cylindrical copper chamber are diameter 160 mm and length 380 mm. The waveguide is joined to the chamber in the center through a rectangular opening with dimensions 45×90 mm^2, oriented so that the smaller dimension is parallel to the cylindrical axis of the chamber; the ends of the cylinder are closed with a brass grid with spacing 5×5 mm^2. The midplane of the chamber has several diagnostic openings in addition to the input from the waveguide. Figure 1 also shows the location of the acoustic microphones used for measurements in the frequency range 20–20000 Hz.

The diagnostic complex consisted of a system for making calorimetric measurements of the microwave power and the LP power; a system for optical and pyrometric measurements of the LP temperature; a color video camera and video recorder, with subsequent digitization of the LP images in the visible waveband; a thermal energy device to obtain infrared images of the LP and measurements of the microwave distribution in the discharge chamber; probes; and a thermocouple. The acoustic measurements were performed with a precise robotron 00024 noise meter calibrated with the input signal to a digital C9-8 oscilloscope with subsequent processing on an IBM PC.

In the experiments, after initiation the steady discharge can exist in three different forms (see Fig. 2):

I. A spheroidal LP isolated from the walls of the discharge chamber, with a typical size of 80 mm.

II. An LP in contact with the hemispherical upper metal wall of the discharge chamber, typically 20 mm in dimension.

III. An LP in contact with an insulating upper quartz wall, located in the center of the discharge chamber. In this case two spheroidal LPs with typical dimension 20 mm were generally present.

Sound was excited in two ways: by means of the variable electric potential applied to the two insulated copper electrodes in contact with the LP (Fig. 3); or by modulating the power of the magnetron supplying the discharge.

3. SOUND EXCITATION IN AN LP

3.1. Let us analyze the process of sound excitation in an LP when the power of the microwave field maintaining the discharge is modulated. When an LP radiates the role of the charged particles (electrons) reduces mainly to absorbing the microwave energy, although they have a negligible effect on the movement of the medium. To describe the sound oscilla-
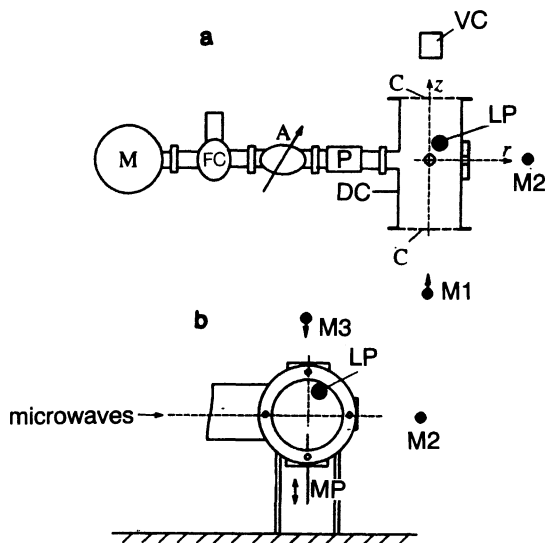
FIG. 1. a) General schematic of the apparatus: M) magnetron; FC) ferrite circulator; A) attenuator; P) protective section; DC) discharge chamber; g) end grids. b) Disposition of the diagnostics; m) measuring microphones; VC) video camera; p) movable probe and discharge initiator.

tions of an LP we will therefore use the system of hydrodynamic equations for the neutral component of the gas:

$$\frac{\partial \rho}{\partial t} + \mathrm{div}\ \rho \mathbf{v} = 0, \quad \rho \frac{d\mathbf{v}}{dt} = -\nabla p, \quad \frac{3}{2}\frac{\rho}{m}\frac{dT}{dt} + \frac{\rho T}{m}\ \mathrm{div}\ \mathbf{v} = q,$$
(1)

where ρ is the air density, q is the heat produced per unit volume, and the rest of the notation is standard. We have omitted the effects of viscosity and thermal conduction in this system of equations. When the hydrodynamic approximation is applicable ($\omega \ll \nu$, where ω is the oscillation frequency and ν is the collision frequency with the neutral particles) these phenomena have little effect on the sound excitation process of interest to us. Note that for $\omega \ll \nu$ the sound damping mechanism due to friction between the neutral particles and the charged particles is unimportant.[11]

We assumed that the heat release has a constant term and another one which varies harmonically with time:

$$q(\mathbf{r},t) = q_0(\mathbf{r}) + q_1(\mathbf{r})\exp(-i\omega t).$$

Linearizing Eqs. (1) in terms of a small perturbation produced by the modulation q, we arrive at the following wave equation:

$$\rho_0 \nabla \left(\frac{1}{\rho_0}\ \nabla \tilde{p}_1\right) + \frac{\omega^2}{c^2}\ \tilde{p}_1 = \frac{2}{3}\frac{i\omega}{c^2}\ q_1,$$
(2)

where c is the speed of sound. The homogeneous form of the equation corresponding to (2) can be found, e.g., in Ref. 12.

Without pretending to obtain an exact quantitative description of the phenomenon, let us consider a simplified model that nevertheless allows us to exhibit some typical qualitative behavior. We assume that the LP is spherically symmetric (with radius r_0) and that the transition from hot ionized gas (temperature T_{in}) to cold unionized gas (temperature T_{ex}) occurs in the layer with thickness $a \ll r_0$. We will
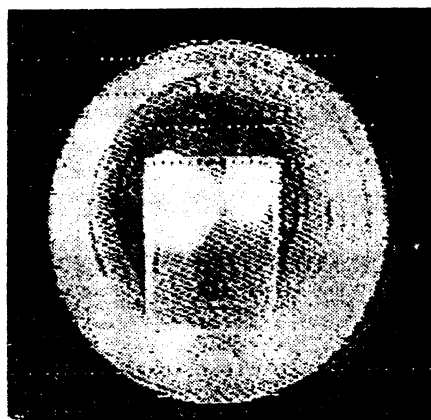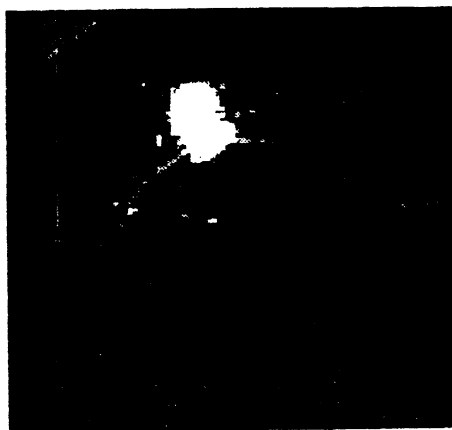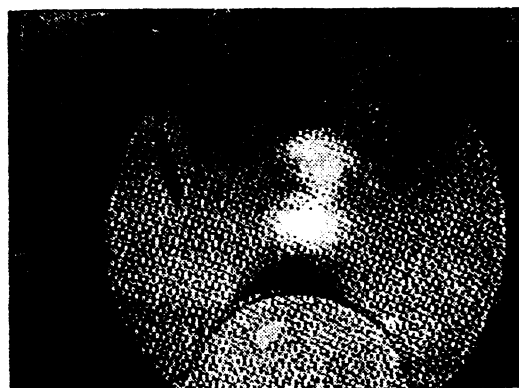
FIG. 2. Different types of LP: a) separated from the discharge chamber walls (type I); b) in contact with a metal chamber wall (type II); c) in contact with a quartz wall (type III).

also assume that the heat release is concentrated in the boundary of the LP in a shell of thickness $b < a$. This model is in qualitative agreement with the air temperature profiles observed experimentally (T_{in} reaches 4500 K) and the electric potential profiles of the microwave field (the typical skin depth of the field is 1 cm). Note that a similar model gives a good description of the properties of microwave discharges in the atmosphere.[4,13,14]

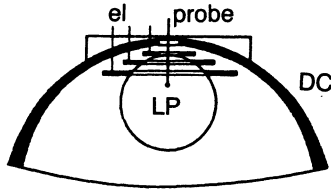The spherically symmetric solution of (2) which satisfies

FIG. 3. LP in contact with insulated copper electrodes: DC) discharge chamber; el) electrodes; p) movable probe.

FIG. 4. Contour of integration.

the condition of boundedness in the limit $r \to 0$ and the radiation condition in the limit $r \to \infty$ assumes the form

$$\bar{p}_1(r) = -p_{ex}(r) \int_0^r dr' p_{in}(r') f(r')/w(r')$$

$$+ p_{in}(r) \int_r^\infty dr' p_{ex}(r') f(r')/w(r'), \qquad (3)$$

where $f(r) = (2/3)(i\omega/c^2) q_1(r)$; p_{in} and p_{ex} are the solutions of the homogeneous equation (2) satisfying the above boundary conditions. It is convenient to choose them in a form so that in the inner region the first term goes over to $j_0(r\omega/c_{in})$, while in the outer region the second term goes over to $h_0^{(1)}(r\omega/c_{ex})$; w is the functional determinant. Here j_0 and h_0 are the spherical Bessel and Hankel functions respectively.

3.2. Our aim is to calculate the power of the sound emitted by the LP. For this it suffices to know

$$\bar{p}_1(r)_{r \to \infty} \approx -p_{ex}(r) \int_0^\infty dr' p_{in}(r') f(r')/w(r'). \qquad (4)$$

The integral on the right-hand side of (4) can be evaluated analytically in two limiting cases: high-frequency oscillations with wavelength much less than the thickness b of the shell in which heat is released, and low-frequency oscillations whose wavelength is much greater than the size of the transition region, $a > b$.

We use the quasiclassical approximation to describe short-wavelength oscillations. The homogeneous equation (2) assumes the usual form suitable for introducing the quasiclassical approximation if we go over to the new variable $\eta = \int^r dr \rho_0/r^2$:

$$\frac{d^2 p}{d\eta^2} + \kappa^2 p = 0, \qquad (5)$$

where $\kappa(\eta) = kr^2/\rho_0$ and $k = \omega/c$ is the sound wave number. From (5) we find

$$p_{ex}(r) = -i \frac{1}{r\omega} \left(\frac{c_{ex}^3}{c_{in}} \right)^{1/2} \exp\left(i\omega \int^r dr/c \right),$$

$$p_{in}(r) = \frac{1}{r\omega} \left(\frac{c_{ex}^3}{c_{in}} \right)^{1/2} \sin\left(\omega \int^r dr/c \right).$$

Here the functional determinant is found to be equal to
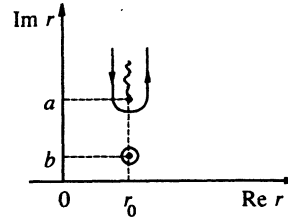
$$w = -i \frac{c_{ex}^3}{\omega r^2 c^2},$$

and expression (4) assumes the form

$$\bar{p}_1 = -i \frac{\omega^2}{3c_{ex}^2} p_{ex} \int_0^\infty dr \; r^2 p_{ex}(r) q_1(r). \qquad (6)$$

In order to evaluate the integral in (6) analytically, we must specify the spatial dependence of $c(r)$ and $q_1(r)$. We choose the simplest forms consistent with the above assumptions:

$$q_1(r) = \frac{Qb}{4\pi^2 r_0^2((r-r_0)^2 + b^2)}, \qquad c = \sqrt{\frac{5}{3} \frac{T(r)}{m}},$$

where

$$T(r) = \frac{1}{2} \left[(T_{in} + T_{ex}) + (T_{ex} - T_{in}) \frac{r - r_0}{\sqrt{(r-r_0)^2 + a^2}} \right],$$

here Q is the amplitude of the modulation in the magnetron power and m is the mass of a gas molecule.

The principal contribution to the integral comes from the region of the transition between the LP and the cold gas, within which the heat release is localized. Taking into account the conditions $r_0 \gg a > b$, we can rewrite the lower limit of the integration in (6) as $-\infty$ and shift the integration contour from the real axis into the upper half-plane of the complex variable r, where the solution p_{ex} decays exponentially. The value of the integral in (6) is determined by the properties of the integrand: the pole $q_1(r)$ at the point $r = r_0 + ib$ and the cut leaving the branch point $(r = r_0 + ia)$ of the functions $T(r)$ and $c(r)$ (see Fig. 4) Since we assume $a > b$, the pole is located close to the real axis and its contribution dominates:

$$\bar{p}_1(r) = -\frac{i2^{5/4} Q C_1 \sin \Phi}{12\pi r r_0 \sqrt{c_{in} c_{ex}}} \exp\left(i\omega \int^r \frac{dr}{c} - A \right), \qquad (7)$$

where

$$C_1 = \left(\frac{1 - \beta^2}{(1+\tau)^2 - 4\tau\beta} \right)^{1/8}, \qquad \Phi = \Phi_1 + \Phi_2,$$

$$\Phi_1 = \frac{1}{4} \arctan\left(\frac{1-\tau}{1+\tau} \frac{\beta}{\sqrt{1-\beta^2}} \right),$$

$$\Phi_2 = -\frac{\sqrt{2}\omega b}{c_{in}} \operatorname{Im} J, \qquad A = \frac{\sqrt{2}\omega b}{c_{in}} \operatorname{Re} J,$$

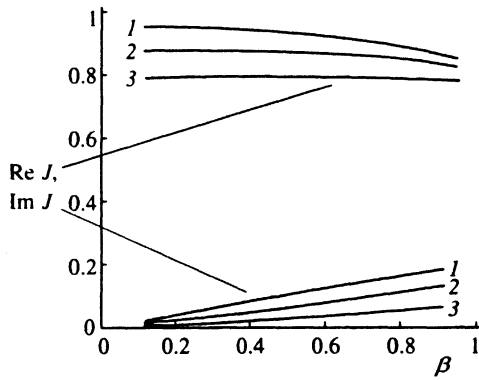$$J = \int_0^1 \frac{d\xi}{\left(1 + \tau - i(1-\tau) \frac{\xi}{\sqrt{\beta^{-2} - \xi^2}} \right)^{1/2}},$$

FIG. 5. Calculation of $\text{Re }J$ and $\text{Im }J$ as functions of β for different values of τ. 1) 0.1; 2) 0.3; 3) 0.6.

$\tau = T_{ex}/T_{in}$, $\beta = b/a$. Figure 5 shows the calculated behavior of the imaginary and real parts of J as a function of β for different values of τ.

The flux density of the acoustic energy, as is well known, is equal to

$$S = \frac{|\tilde{p}_1|^2}{2\rho c}.\tag{8}$$

Taking into account (6) and (8) we find the total power radiated by the LP:

$$W = \frac{\sqrt{2}Q^2 C_1^2}{30\pi c_{in}p_0 r_0^2}\sin^2\Phi e^{-2A}.\tag{9}$$

Here p_0 is the pressure of the surrounding air and c_{in} is the sound speed at the center of the LP. In this expression it is worth noting that the exponential factor cuts off the emission when the typical wavelength of the oscillations is less than the thickness of the shell in which heat is released.

The LP boundary emits both outgoing and incoming sound waves. The latter also become outgoing after reflecting from the center. The interference between them and the waves emitted outward directly is taken into account in (9) through the oscillating factor.

3.3. Now let us consider the opposite limiting case of low-frequency oscillations whose wavelength is much greater than both the thickness of the heat-emitting shell and the size of the transition layer at the boundary of the LP. To analyze these oscillations we can set

$$q_1(r) = \frac{Q}{4\pi r_0^2}\delta(r - r_0), \quad T(r) = \begin{cases} T_{in} & r < r_0 \\ T_{ex} & r > r_0. \end{cases}$$

In order to solve Eq. (2), we can proceed as we did before and use expression (4), in which we now set

$$p_{ex}(r) = -i\frac{c_{ex}}{r\omega}\exp\left(i\frac{r\omega}{c_{ex}}\right), \quad (r > r_0), \quad p_{in}(r) = \begin{cases} \dfrac{c_{in}}{r\omega}\sin\left(\dfrac{r\omega}{c_{in}}\right), & (r < r_0) \\[2ex] \dfrac{c_{ex}}{r\omega}\left(\mathcal{A}\sin\left(\dfrac{r\omega}{c_{ex}}\right) + \mathcal{B}\cos\left(\dfrac{r\omega}{c_{ex}}\right)\right), & (r > r_0), \end{cases}$$

$$\mathcal{A} = \frac{\sin z_{in}(z_{ex}\sin z_{ex} + \cos z_{ex}) + \tau^{-1}\cos z_{ex}(z_{in}\cos z_{in} - \sin z_{in})}{z_{ex}\sqrt{\tau}},$$

$$\mathcal{B} = \frac{\sin z_{in}(z_{ex}\cos z_{ex} - \sin z_{ex}) - \tau^{-1}\sin z_{ex}(z_{in}\cos z_{in} - \sin z_{in})}{z_{ex}\sqrt{\tau}},\tag{10}$$

$$w = -i\frac{(A - iB)c_{ex}^3}{\omega c^2(r)}, \quad z_{in} = \frac{r_0\omega}{c_{in}}, \quad z_{ex} = \frac{r_0\omega}{c_{ex}}.$$

By means of these expressions we find the pressure oscillations in the external region ($r > r_0$):

$$\tilde{p}_1(r) = -\frac{i}{6\pi}\frac{c_{in}Q\sin z_{in}}{c_{ex}^2 r r_0(\mathcal{A} - i\mathcal{B})}\exp\left(i\frac{r\omega}{c_{ex}}\right),\tag{11}$$

and the total radiated power of the LP:

$$W = \frac{Q^2 C_2}{30\pi p_0 c_{ex}r_0^2},\tag{12}$$

where

$$C_2 = \frac{z_{ex}^2\sin^2 z_{in}}{z_{ex}^2\sin^2 z_{in} + [\sin z_{in} + \tau^{-1}[z_{in}\cos z_{in} - \sin z_{in}]]^2}.$$

Comparison of (12) and (9) shows that when the frequency of the oscillations decreases the strong exponential behavior of w as a function of ω drops out. In its place a smooth dependence appears due to the presence of eigenmodes[1] of the LP with a sharp boundary. Specifically, the dispersion relation (3) of these oscillations can be written in the form $\mathcal{A} - i\mathcal{B} = 0$. Then in the expression for p_{in} [see Eq. (10)] the infinite wave will no longer be present, and it becomes identical with the expression for the eigenmodes
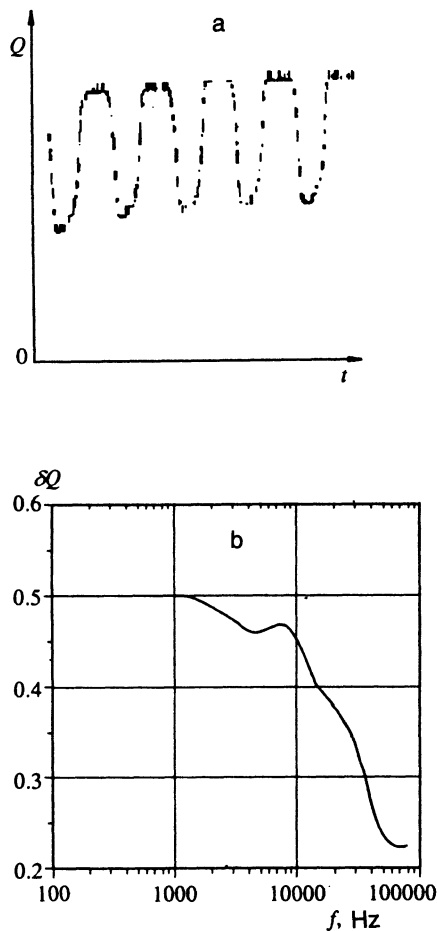
FIG. 6. Modulation of the magnetron power: a) typical oscilloscope trace of the signal from the microwave detector with a sinusoidal modulation of frequency 5 kHz; b) modulation depth of the power as a function of the modulation frequency.
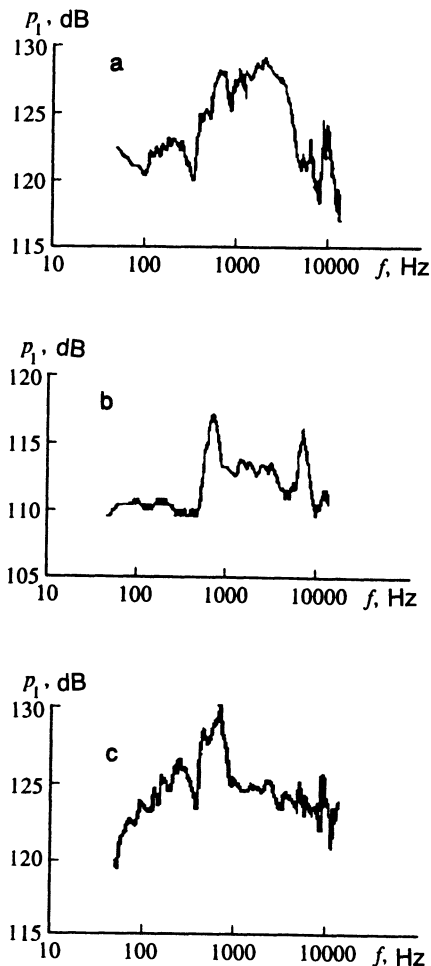

FIG. 7. Sound intensity detected by microphone M1 as a function of the modulation frequency for the three types of LP: a) type I; b) type II; c) type III.

[see Eq. (3)]. Because the damping rate of eigenmodes is quite large, the associated resonances in the dependence of W on ω are found to be smeared out.

4. EXPERIMENTS ON SOUND EXCITATION

4.1. Let us discuss experiments on sound excitation due to modulation of the microwave power. A rumbling sound associated with pulsations in the power supply of the magnetron (the source of the microwave power) was continually recorded in our experiments. It can be assumed that in most other experiments with steady discharges in the atmosphere the observable acoustic phenomena resulted from pulsations in the power circuit. We have employed driven controlled modulation of the microwave power to generate intense noise. Figure 6 shows an oscilloscope trace of the signal from the microwave detector, which recorded the microwave power level in the discharge chamber. The same figure shows the modulation depth of the microwave power as a function of the modulation frequency. Experiments were carried out in the range of modulation frequencies for which the modulation depth depended weakly on frequency. Note that the signal from the microwave detector had a complicated shape and it varied with the modulation frequency.

The power modulation frequency determined the frequency at the sound frequency ω and the modulation depth Q determined the intensity. In the experiments we recorded the sound intensity as a function of the modulation frequency. We used several microphones positioned in various places (Fig. 1). The modulation frequency was varied continuously through six seconds, during which the properties of the LP did not change in general.

In Fig. 7 the frequency dependence of the sound intensity is shown for the three forms of LP, as recorded by microphone M1 (see Fig. 1), located at a distance of 30 cm laterally from the LP. The sound intensity p_1 was measured in dB, using the following calibration relation for the device employed in the experiments:

$$p_1(\text{dB}) = 20 \lg(\bar{p}_1/2 \cdot 10^{-5}(\text{Pa})), \qquad (13)$$

where $\bar{p}_1$ is the effective value of the pressure oscillation amplitude in the sound wave. The intensity of the parasitic noise (from the operation of the fan unit in the magnetron power supply, etc.) was less than 85 dB and was considerably less than the intensity of the LP noise that was produced.

What general features associated with sound generation by the LP can be discerned in the experiment? First, the

spectral properties depend sensitively on the form of the LP. Thus, while the sound intensity begins to fall fairly rapidly for frequencies above 2 kHz for type I LPs, for types II and III this occurs at frequencies above 10 kHz. Second, for all types of LP in the range below 1 kHz, despite the presence of small-scale variations the sound intensity typically increases with frequency. Third, the complicated "jagged" structure of the frequency dependence of the sound frequency is observed for all types of LP, but especially for type I.

In Fig. 8 the calculated and experimental behavior of the sound intensity is plotted versus frequency.[2] Cases 1 and 2 in Figs. 8a and 8b were obtained using Eqs. (7) and (11) respectively. The first of these equations is valid in the high-frequency region and the second in the region of low frequency. Of the two equations (7) and (11), the smaller values of $\tilde{p}_1$ are given by that which is valid in a given region. We can therefore approximate the frequency dependence of the whole frequency range of interest reasonably well by using the extrapolation

$$\tilde{p}_1 = (|\tilde{p}_{11}|^{-1} + |\tilde{p}_{12}|^{-1})^{-1},$$

where the values of $\tilde{p}_{11}$ are calculated using (7) and those of $\tilde{p}_{12}$ are calculated using (11). The latter expression was used to calculate the trace in Fig. 8c.

Figures 8a and b differ in the size of the LP. For a large LP of dimension $r_0 = 4$ cm (corresponding to a type-I LP) a dropoff in the frequency dependence is observable in the range of frequencies $\sim 10^4$ Hz. With smaller LPs of radius $r_0 = 1$ cm (corresponding to LPs of types II and III) Fig. 7 shows no dropoff. Presumably it has shifted to the region of larger frequencies.

Figure 8c shows that the agreement between theory and experiment is completely satisfactory over the entire frequency range studied. Thus, although the theoretical analysis makes no pretense at a quantitative description of the experiment, comparison of Figs. 7 and 8 shows that the model describes not only the qualitative features of the phenomenon mentioned above, but also the main quantitative features: the intensity and the value of the frequency at which the curve "drops off."

As shown by the calculations, the observed frequency dependence of the sound emitted at high frequencies can be related to interference effects when the modulation frequency is high (the smooth-boundary model) and to the presence of damped eigenmodes of the LP at low frequency (the sharp-boundary model). Although both factors have been taken into account in the theoretical model, in view of its ideal nature one can scarcely expect exact agreement with experiment. Specifically, in the model the LP was taken to be spherically symmetric. In this case interference effects are particularly strong; they cause the emitted intensity to vanish at several discrete values of the frequency [cf. Eqs. (9) and (12)]. However, real LPs, even in the states which are separated from the walls (type I) are all quite asymmetric. This should cause the waves emitted by different portions of the LP boundary to be desynchronized. As a result, the experimental frequency dependence should become smoother.

In analyzing the acoustic eigenmodes of an LP (see Appendix) it is assumed that the plasma exists in free space.
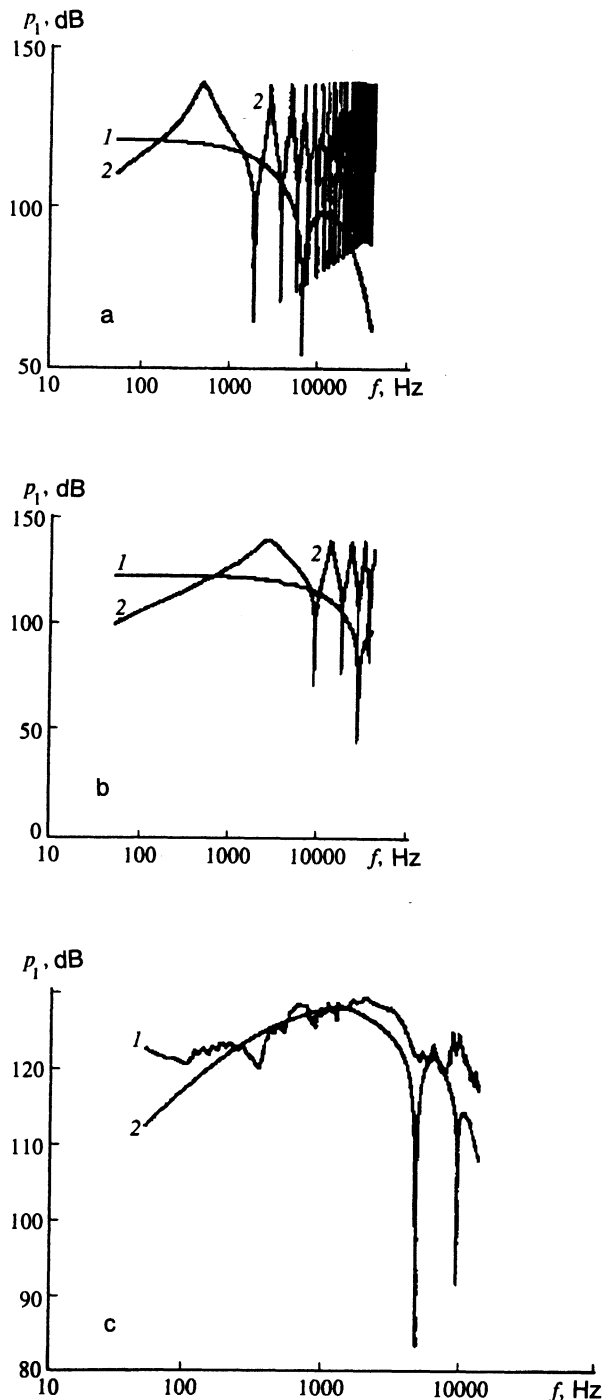

FIG. 8. Calculation of the sound intensity detected by microphone M1 using the following equations: 1) (7); 2) (11) with the following parameters: a) $r_0 = 4$ cm, $R = 6$ cm, $a = 2$ cm, $\beta = 0.9$, $Q = 2$ kW, $\tau = 0.2$; b) $r_0 = 1$ cm, $R = 10$ cm, $a = 0.4$ cm, $\beta = 0.9$, $Q = 1$ kW, $\tau = 0.3$; c) comparison of experiment E and calculation C with the following parameters: $r_0 = 2$ cm, $R = 5$ cm, $a = 0.6$ cm, $\beta = 0.9$, $Q = 2.5$ kW, $\tau = 0.35$.

The boundedness of the volume in which the LP is observed should be reflected substantially in the frequency spectrum of the resulting sound. By virtue of the small size of the LP one can expect that it will reflect the sound-wave spectrum of the discharge chamber. The effect of geometry was particularly noticeable in the low-frequency part of the spectrum. Thus, introducing additional massive insulating end
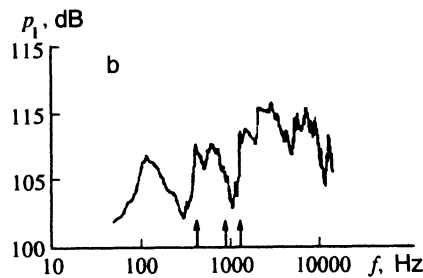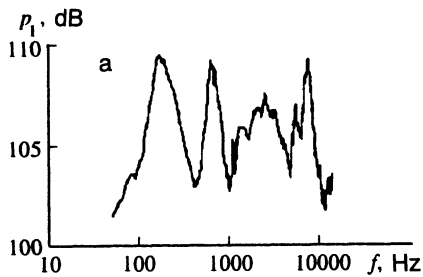
FIG. 9. Intensity with which sound is produced by an LP of type III, measured by microphone M3: a) with open ends; b) with closed ends. The arrows indicate the first three sound resonances along the axis of the discharge chamber.
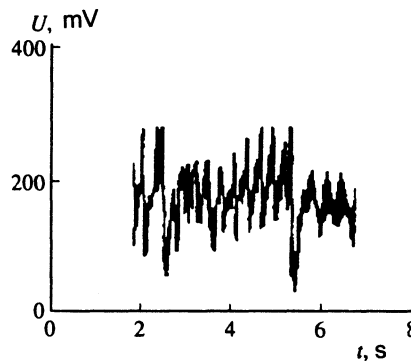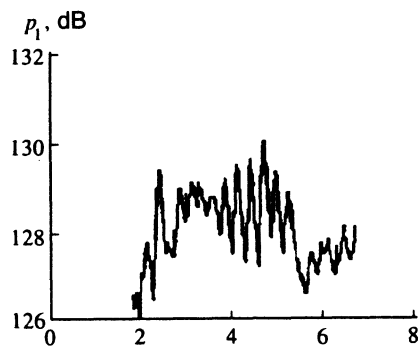

FIG. 10. Oscilloscope trace of the sound p_1 at frequency 1.1 kHz measured by microphone M2 and the voltage U of the microwave detector for an LP of type II.

walls caused the low-frequency maxima in the spectrum to undergo a shift (Fig. 9).

In conclusion we note several interesting observations made in the course of this work. Whereas LPs of the form I and III are quite quiescent, those of type II can radiate irregular crackles associated with oscillations of the LP as a whole in space. Figure 10 displays the oscilloscope trace in time of the sound intensity (at frequency 1.1 kHz) and the intensity of the microwave field in the discharge chamber, measured by a silicon microwave detector. Changing the position and shape of the LP changes the profile of the microwave field in the discharge chamber, which is accompanied by simultaneous changes in the sound intensity.

If we feed the amplified signal from an ordinary microphone into the modulator used for the magnetron power, ordinary human speech is reproduced without significant distortions. When the microphone is moved close to the discharge chamber, acoustic feedback occurs, resulting in the generation of sound at different eigenfrequencies when the position and orientation are changed. As a rule, frequencies in the kHz band were excited. An interesting property of these experiments with LPs of type I is that the alteration in the shape of the LP is visible to the naked eye. Under certain circumstances the LP shape becomes more spherical; in others it is highly distorted.

Let us estimate the possibility of acoustic effects on an LP in our experiments when the pressure oscillation amplitude $\bar{p}$ can reach a value of order 100 Pa and the associated oscillation velocity satisfies $\bar{v} = \bar{p}/\rho c \approx 0.3$ m/s. Estimating the acoustic pressure by $P = \bar{p}\bar{v}/c$ yields the value 0.1 Pa, which is comparable with the effect on the LP of the buoyant force due to Archimedes' principle. Furthermore, the magni-

tude of the velocity $\bar{v}$ is of the same order as the measured convective velocities of the gas inside the LP. These experiments show that the prospects for using sound to stabilize plasma structures in space in the atmosphere are realistic.

4.2. Let us briefly discuss experiments in which sound was excited by applying a variable bias to the electrodes. In these experiments we used a type-I LP. Figure 11 shows how the current between the ring electrodes varies (Fig. 3) as a function of the constant voltage applied to them. Along with the constant voltage we also fed in a variable one with amplitude of up to 100 V and frequency from 20 to 20000 Hz. We also applied permanent magnets with field strength of about 200 G to the LP. A weak acoustic emission was observed, at the level of the parasitic noise (85 dB), with a maximum near 1 kHz when the maximum amplitude of the variable field was 100 V. Supplying a variable bias or bringing a magnet near did not lead to any fundamental change in the noise intensity.

These experiments confirm the conclusions of the theory of Timofeev[15] regarding the weak coupling between electrical oscillations and oscillations of the gas pressure under LP conditions. In Ref. 15 it was shown that variable electric fields produced by external sources give most of their energy to highly damped ion acoustic waves. On the other hand, a small fraction of the energy goes into sound, comparable with the degree of ionization of the gas.

5. CONCLUSION

Thus, in the present work we have studied the phenomenon of sound generation in an LP when the power of the
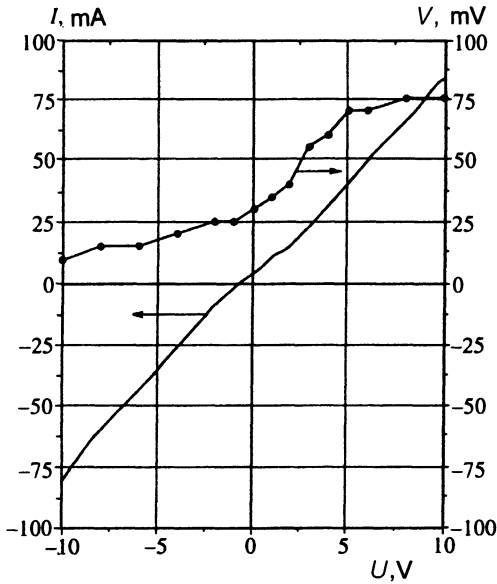
FIG. 11. Current I between external (zero-potential) and intermediate (variable potential) copper ring-shaped electrodes (see Fig. 3) and a probe with floating potential V in the plasma (LP) as a function of the voltage drop between the electrodes.

microwave maintaining the discharge is modulated. We have determined the frequency dependence of the sound intensity emitted by the LP. As the modulation frequency increases the intensity first grows rather slowly and then drops off sharply. Small-scale variations are superimposed on this dependence. This behavior of the frequency dependence can be explained using the model of a spherically symmetric LP with a thin transition layer between the plasma and the cold gas. We have analyzed two limiting cases in which oscillations are excited with a wavelength much less than or much greater than the thickness of the transition layer. The long-wavelength oscillations correspond to the growing part of the frequency dependence, and the short-wavelength oscillations correspond to the decaying part. The value of the frequency at which the dropoff in the frequency depends begins and the characteristic scale of this decay agree with the experimental values. There is order-of-magnitude agreement between the experimental and calculated sound intensity emitted by an LP. The small-scale variations on the frequency dependence are explained by interference effects and the excitation of damped eigenmodes of the LP (the damping is due to leakage of acoustic energy out of the LP).

We wish to thank Zh. F. Lyaitner, É. A. Manykin, and P. Handel for useful comments.

APPENDIX

The eigenmodes of an LP (if they exist) should be described by the homogeneous form of Eq. (2). In the case of a spherically symmetric LP its solution takes the form

$$p_1(\mathbf{r}) = e^{-i\omega t} R(r) Y_{mn}(\cos\theta) e^{im\varphi},$$

where θ and φ are the angles in spherical coordinates and Y_{mn} are the associated Legendre polynomials.

Carrying out separation of variables and transforming from r to the new variable $\eta = \int^r dr(\rho(r)/r^2)$, we find for the radial function $R(r)$ the equation

$$R''_{\eta\eta} + \left(\frac{\omega^2 r^4}{c^2\rho^2} - \frac{n(n+1)r^2}{\rho^2} \right) R = 0. \tag{A1}$$

This equation is an extension of (5) to the general case of nonaxisymmetric oscillations.

Equation (A1) can conveniently be viewed as a Schrödinger equation describing the motion of a particle in the potential

$$U = -\frac{\omega^2 r^4}{c^2\rho^2} + \frac{n(n+1)r^2}{\rho^2}.$$

This equation may have eigenmodes if the transparency region where $U < 0$ holds is bounded.

For spherically symmetric solutions the transparency region occupies the entire semiaxis $0 \leqslant r < \infty$ (here $-\infty < \eta \leqslant 0$). In an LP with a temperature that decays monotonically in radius (increasing density) a region of opacity develops near the center, but the transparency region remains unbounded in r. Note that the use of the variable η means that we view the escape of oscillations from the LP ($r \to \infty$) as a fall to the center.

Thus, we arrive at the conclusion that in an LP with a temperature that decreases monotonically in radius there are no eigenmodes with Im $\omega = 0$. On the other hand, in view of their nonuniformity LPs can have damped eigenmodes. The damping is due to leakage of the acoustic energy. The damping rate is smallest in an LP with a sharp boundary, for which the reflection coefficient is largest.

Consider an LP with a temperature jump at the boundary (see Sec. 3.3). Spherically symmetric solutions of the wave equation take the form

$$R(r) = \begin{cases} j_0\left(\dfrac{r\omega}{c_{\rm in}}\right), & r < r_0 \\[2mm] C h_0^{(1)}\left(\dfrac{r\omega}{c_{\rm ex}}\right), & r > r_0. \end{cases} \tag{A2}$$

The requirements that the quantities R and $(r^2 dR/dr)/\rho$ be continuous at the LP boundary enable us to determine the constant C in (A2) and the eigenfrequency. For the latter we find the dispersion relation

$$\operatorname{ctg} z_{\rm in} = \frac{1}{z_{\rm in}}(1-\tau) + i\sqrt{\tau}. \tag{A3}$$

Its approximation solutions in the limit $\tau \ll 1$ take the form

$$\omega \approx \frac{c_{\rm in}}{2r_0}\sqrt{3\tau}(1 - i\sqrt{3})$$

for the ground state ($n = 0$) and

$$\omega \approx \frac{c_{\rm in}}{2r_0}\left[\left(n + \frac{1}{2}\right)\pi - i\sqrt{\tau}\right]$$

for the higher radial modes ($n \gg 1$).

Note that when the temperature drop at the LP boundary is large ($\tau \ll 1$) the damping rate is small (Im $\omega \ll$ Re ω) and these oscillations are close to the usual eigenmodes.

[1] By eigenmodes we mean those oscillations whose spatial structure is described by solutions of the homogeneous form of Eq. (2) which satisfy the condition of finiteness at the origin and the radiation condition at infinity. On account of the leakage of acoustic energy from an LP these oscillations are found to be damped. The eigenmodes are studied in the Appendix.

[2] The sound attenuation that results when the measuring microphone is moved away from the LP can be taken into account by introducing an effective distance $r = R$ in Eqs. (7) and (11). In order to determine R for microphone $M1$ we have assumed that the sound leaving through a lateral hole of the chamber is detected without attenuation, and its intensity is reduced in proportion to the ratio of the LP surface to the area of the two lateral openings of the discharge chamber.

[1] R. P. Ouellette, M. Barrieux, P. Cheremisinoff et al., Industrial Applications of Low-Temperature Plasmas [Russian translation], Énergoatomizdat, Moscow (1983).

[2] S. V. Dresvin, Introduction to the Theory and Calculation of High-Frequency Plasmatrons [in Russian], Énergoatomizdat, Leningrad (1991).

[3] S. V. Dresvin and V. D. Rusanov, HF and Microwave Plasmatrons Vol. 6 [in Russian], Nauka, Novosibirsk (1992).

[4] Yu. P. Raizer, Gas-Discharge Physics, Springer, New York (1991).

[5] P. L. Kapitsa, Dokl. Akad. Nauk SSSR 101, 245 (1955); Zh. Eksp. Teor. Fiz. 30, 973 (1970) [Sov. Phys. JETP 57, 1801 (1969)].

[6] J. R. Powell and D. Finkelstein, Am. Sci. 58, 262 (1970) [see J. D. Barry, Ball Lightning and Bead Lightning, Plenum, New York (1980)].

[7] P. H. Handel, in Science of Ball Lightning (Fire Ball), Y. H. Ohtsuki (ed.), World Scientific, Singapore (1989).

[8] Y. H. Ohtsuki and H. Ofuruton, Nature 350, 139 (1991).

[9] B. P. Milyus, in 8th International Conf. on Low-Temperature Plasma Generators, Novosibirsk (1980).

[10] G. A. Galechyan, Priroda No. 3, 65 (1994).

[11] U. Ingard and K. W. Gentle, Phys. Fluids 12, 396 (1969).

[12] D. I. Blokhintsev, Acoustics of Nonuniform Moving Media [in Russian], Nauka, Moscow (1981).

[13] Y. P. Raizer, Laser-Induced Discharge Phenomena, Consultants Bureau, New York (1977).

[14] Yu. P. Raizer, Foundations of the Modern Physics of Gas-Discharge Processes [in Russian], Nauka, Moscow (1980).

[15] A. V. Timofeev, Fiz. Plazmy 20, (1994) [Plasma Phys. Repts.] (in press).

Translated by David L. Book